Title

Antimicrobial production by perifollicular dermal preadipocytes is essential to the pathophysiology of acne

Journal

Science Translational Medicine, 14(632)

ISSN

1946-6234

Authors

O'Neill, Alan M
Liggins, Marc C
Seidman, Jason S
et al.

Publication Date

2022-02-16

DOI

10.1126/scitranslmed.abh1478

Peer reviewed

HHS Public Access

Author manuscript

Sci Transl Med. Author manuscript; available in PMC 2023 January 30.

Published in final edited form as:

Sci Transl Med. 2022 February 16; 14(632): eabh1478. doi:10.1126/scitranslmed.abh1478.

Antimicrobial production by perifollicular dermal preadipocytes is essential to the pathophysiology of acne

Alan M. O'Neill[1,†], **Marc C. Liggins**[1,†], **Jason S. Seidman**[2], **Tran H. Do**[3], **Fengwu Li**[1], **Kellen J. Cavagnero**[1], **Tatsuya Dokoshi**[1], **Joyce Y. Cheng**[1], **Faiza Shafiq**[1], **Tissa R. Hata**[1], **Johann E. Gudjonsson**[4], **Robert L. Modlin**[3], **Richard L. Gallo**[1,*]

[1]Department of Dermatology, University of California, San Diego, La Jolla, CA 92093, USA.

[2]Department of Cellular and Molecular Medicine, University of California, San Diego, La Jolla, CA 92093, USA.

[3]Division of Dermatology, University of California, Los Angeles, Los Angeles, CA 90095, USA.

[4]Department of Dermatology, University of Michigan, Ann Arbor, MI 48109, USA.

Abstract

Innate immune defense against deep tissue infection by *Staphylococcus aureus* is orchestrated by fibroblasts that become antimicrobial when triggered to differentiate into adipocytes. However, the role of this process in non-infectious human diseases is unknown. To investigate the potential role of adipogenesis by dermal fibroblasts in acne, a disorder triggered by *Cutibacterium acnes*, single-cell RNA sequencing was performed on human acne lesions and mouse skin challenged by *C. acnes*. A transcriptome consistent with adipogenesis was observed within specific fibroblast subsets from human acne and mouse skin lesions infected with *C. acnes*. Perifollicular dermal preadipocytes in human acne and mouse skin lesions showed colocalization of PREF1, an early marker of adipogenesis, and cathelicidin (*Camp*), an antimicrobial peptide. This capacity of *C. acnes* to specifically trigger production of cathelicidin in preadipocytes was dependent on TLR2. Treatment of wild-type mice with retinoic acid (RA) suppressed the capacity of *C. acnes* to form acne-like lesions, inhibited adipogenesis, and enhanced cathelicidin expression in

*Corresponding author. rgallo@health.ucsd.edu.
†These authors contributed equally to this work.

Author contributions: A.M.O. and M.C.L. designed and performed experiments involving scRNA-seq, qPCR, microscopy imaging, and quantitation of human and mouse tissue; performed statistical analysis; prepared figures; and wrote the manuscript. J.S.S. analyzed human and mouse scRNA-seq data and prepared figures in R. T.H.D. wrote the IRB, collected the human acne specimens, performed and analyzed the scRNA-seq data for human acne, and assisted with mouse scRNA-seq. F.L. conducted human and mouse tissue sectioning, staining, and imaging and analyzed data. T.D. and K.J.C. performed experiments, conducted CellChat analysis, and analyzed data. J.Y.C., F.S., and T.R.H. recruited volunteers and obtained human biopsies. J.E.G. recruited volunteers, analyzed data, and contributed to manuscript preparation. R.L.M. analyzed data and contributed to manuscript preparation. R.L.G. conceived, designed, and supervised experimental procedures and prepared the manuscript.

Competing interests: R.L.G. is a cofounder, scientific advisor, and consultant and has equity in MatriSys Bioscience and is a consultant, receives income, and has equity in Sente Inc.

SUPPLEMENTARY MATERIALS
www.science.org/doi/10.1126/scitranslmed.abh1478
Figs. S1 to S6
Table S1
MDAR Reproducibility Checklist
Data file S1
View/request a protocol for this paper from *Bio-protocol*.

preadipocytes, but lesions were unresponsive in *Camp*$^{-/-}$ mice, despite the anti-adipogenic action of RA. Analysis of inflamed skin of acne patients after retinoid treatment also showed enhanced induction of cathelicidin, a previously unknown beneficial effect of retinoids in difficult-to-treat acne. Overall, these data provide evidence that adipogenic fibroblasts are a critical component of the pathogenesis of acne and represent a potential target for therapy.

INTRODUCTION

Acne vulgaris is an inflammatory disease of the pilosebaceous unit that ranks among the most common global skin disorders (1–4). *Cutibacterium acnes* is a common and abundant member of the skin microbiome that contributes to the inflammation associated with acne (1, 2, 4). To understand factors that drive inflammation in acne, numerous studies have examined host-pathogen interactions between *C. acnes* and local cell types, including keratinocytes, sebocytes, and leukocytes (1, 2, 4–7). However, the pathophysiology of acne remains poorly understood.

The primary anatomical site for development of disease in acne is the specialized physical and immunological barrier of the epithelium within the hair follicle. Under healthy conditions, this epithelium consists of several keratinocyte layers that function as a physical barrier against microbial penetration while also promoting an immunotolerant state in response to constant exposure to microbes (6, 8). In hair follicles, dense *C. acnes* colonization within the less stratified and deeper region of pilosebaceous units presents a specific challenge for the skin. Healthy follicles tolerate the presence of *C. acnes*, but disease conditions in acne promote the capacity of *C. acnes* and its metabolic products to interact with perifollicular cells, stimulate inflammation, and promote the development of acne lesions.

The responses of classical immune and epithelial cells have been evaluated extensively in inflammatory skin disorders such as acne, but the participation of dermal fibroblasts has been less well investigated. Recent observations characterizing the response to *Staphylococcus aureus* skin invasion found that fibroblasts can undergo localized proliferation and differentiation into a preadipocyte lineage, a process dubbed reactive adipogenesis (9–11). Reactive adipogenesis is characterized by elevated expression of preadipocyte factor 1 (PREF1/DLK1) during preadipocyte proliferation. This response provides host defense as it is accompanied by an acute and transient increase of the expression of the antimicrobial peptide cathelicidin (*Camp*) as well as other genes with immunologic functions (10, 12, 13). Cathelicidin expression during reactive adipogenesis limits bacterial growth because impairment of reactive adipogenesis or deletion of *Camp* from cultured fibroblasts results in increased *S. aureus* growth (9, 10, 12, 14). Furthermore, recent studies have shown that reactive adipogenesis takes place in the gut in response to injury, and suppression of this response led to increased penetration of microbial products into the bloodstream and alteration of disease severity (10, 12–15). Thus, current findings in the skin and the gut suggest that fibroblasts in the subepithelial stroma play an important but previously underappreciated immune defense function.

In this study, we sought to better understand the role of fibroblasts in acne. We show that dermal fibroblasts in human acne lesions display a response consistent with reactive adipogenesis. This process could be modeled in mice in which the development of skin lesions by *C. acnes* was dependent on dermal adipogenesis and modified by retinoid treatment. These data show that dermal perifollicular fibroblasts are a previously unknown part of the pathogenesis of acne.

RESULTS

scRNA-seq of acne biopsies reveals an adipogenic response in distinct fibroblast subsets

To investigate the role of stromal fibroblasts in acne, we collected lesional and nonlesional skin biopsies from six acne patients and conducted single-cell RNA sequencing (scRNA-seq) of the fibroblast transcriptome. Targeted gene expression analysis of the fibroblast populations was based on positive expression of the classic fibroblast marker, platelet-derived growth factor receptor α (*PDGFRA*). This analysis resulted in a uniform manifold approximation and projection (UMAP) plot displaying five distinct fibroblast subsets, designated F0 to F4 (Fig. 1A). Single-cell transcriptomes of the F0, F2, and F4 clusters were more associated with nonlesional skin, whereas F1 and F3 were found to be highly enriched in lesional acne (Fig. 1, B and C). Identification of the top three differentially expressed marker genes indicated diverse functions between subsets (Fig. 1D). The nonlesional F0 subset was characterized by high leptin receptor (*LEPR*) expression, which, when stimulated by adipokines such as leptin, leads to activation of a proadipogenic response (16). The lesional-associated F1 subset was characterized by greater expression of chemokines and matrix metalloproteinases including *MMP1* and *MMP3*. Several of these gene markers were previously shown to be up-regulated in acne lesions by microarray (17, 18). Both nonlesional F2 and F0 subsets represented highly adipogenic clusters, with dramatic enrichment of genes involved in "fat cell differentiation" (Fig. 1E and fig. S1A). This adipogenic gene signature in fibroblasts has been shown to be the hallmark of a process we have termed reactive adipogenesis, an adipogenic and antimicrobial transcriptional program mounted in response to bacterial infection (19). The acne lesional-specific F3 subset was characterized by expression of inflammatory gene sets identified by gene ontology (GO) terms "adaptive immune response" and "regulation of acute inflammatory responses" (Fig. 1E and fig. S1B). Noticeably, the F3 subset also contained several highly expressed lipid-associated genes including apolipoprotein (*APOE*) and phospholipase (*PLA2G2A*) (Fig. 1D). In contrast, subset F4 was atypical and reflected a less adipogenic and inflammatory-like state characterized by high expression of *CRABP1*, normally repressed during differentiation, and asporin (*ASPN*), which restricts transforming growth factor β1 (TGFβ1) activity and mesenchymal stromal cell differentiation (20, 21). Associated with the nonlesional state, we speculated that F4 could represent a nonreactive and/or terminally differentiated fibroblast state (22). To test this, we examined the cell lineages with pseudotimes using Slingshot (23). This revealed two distinct lineages originating from the highly reactive and adipogenic progenitor F0 subset and a transitional F2 subset (Fig. 1F). From F2, lineage 1 branches into the lesional-associated and highly inflammatory subsets F3 and F1, whereas lineage 2 transitions to a less adipogenic and inflammatory terminal F4 population. These results support the conclusion that during acne, a subset or subsets

of fibroblasts are stimulated to begin to differentiate into adipocytes and mount an innate immune defense response.

Antimicrobial expression occurs in the acne perifollicular stroma

Reactive adipogenesis begins with the local stimulation and maturation of fibroblasts that is characterized by the release of antimicrobial peptides and initiation of adipogenesis. To determine whether this process occurs in acne, acne lesional and nonlesional skin sections were stained for the preadipocyte marker PREF1 (10, 12) and the antimicrobial cathelicidin peptide LL-37 encoded by the gene *CAMP*. Strikingly, imaging of the acne lesion showed intense fluorescence staining of PREF1 and cathelicidin in the perifollicular stroma of the acne lesion and within the proximal abscess area characterized by the presence of cellular debris (Fig. 2A). Staining of the perilesional area showed evidence of elevated cathelicidin expression in the dermis, a feature not observed in the control nonlesional skin. *CAMP* expression was validated by quantitative polymerase chain reaction (qPCR), showing a marked increase in *CAMP* mRNA expression in acne skin versus nonlesional skin (Fig. 2B). Confocal microscopy of the perifollicular stroma showed that cathelicidin colocalized with the PREF1 preadipocyte marker (Fig. 2C), a strong indicator of reactive adipogenesis, because *CAMP* is highly expressed by preadipocytes during early differentiation into adipocytes (10). Quantification of cathelicidin fluorescence intensity revealed a greater amount of cathelicidin production in PREF1 preadipocytes compared with PREF1-negative cells, confirming that reactive adipogenesis is occurring in the perifollicular fibroblasts in acne (Fig. 2D). Moreover, cathelicidin staining was minimal in the epidermis and was found to localize below the stratum basale, marked by K14 expression (fig. S2).

The pathophysiology of acne is thought to be driven, in part, by the presence of *C. acnes* within the follicular environment and an epithelial and lymphoid response to bacterial products (24–26). To study dermal reactive adipogenesis in response to *C. acnes*, we used an acne-like mouse model that was generated by intradermal injection of *C. acnes* (27, 28). Consistent with our findings in human acne, mouse dermis adjacent to *C. acnes* injection exhibited markedly increased staining for the preadipocyte marker PREF1 and the mouse antimicrobial cathelicidin ortholog CRAMP (cathelicidin-related antimicrobial peptide) (Fig. 2E). In contrast, mock phosphate-buffered saline (PBS)–infected mice showed sparse staining for PREF1 and CRAMP. Although CRAMP protein increases in the dermis during skin infections due to recruitment of neutrophils and new synthesis by preadipocytes (10, 29), CRAMP colocalized to many cells in the dermis lacking the neutrophil marker GR-1 (Fig. 2F). Transcriptional analysis of *C. acnes*–infected whole tissue was compared over time to mock-infected skin and showed up-regulation of several adipogenic markers, including *Cebpa*, *Cebpb*, *Pref1*, *Adipoq*, and *Camp*, as well as a transcriptional activator of *Camp*, *Hif1a* (Fig. 2G). These data from a murine acne-like mouse model were consistent with our findings in human acne and suggested that reactive adipogenesis occurs as a host immune defense against *C. acnes*.

scRNA-seq reveals proadipogenic and proinflammatory fibroblast subsets in *C. acnes*–infected mice

To better define the localized dermal adipogenic response to *C. acnes* in vivo, we conducted scRNA-seq analysis of whole tissue from mouse skin biopsies after intradermal infection with *C. acnes*. A total of 28,258 sequenced cells from both *C. acnes*–infected and mock-infected skin met quality control standards and were analyzed using unsupervised clustering (Seurat package). Six major cell types were identified and visualized using UMAP (Fig. 3A). Analysis of the *Pdgfra*-positive fibroblast population identified 10 distinct clusters (0 to 9) within the pooled cell samples (Fig. 3B). Further examination revealed that clusters 2, 4, 5, and 6 were highly enriched during *C. acnes* infection (Fig. 3, C and D). Similar to the human acne single-cell dataset, GO terms indicating adipogenesis and immune responses were uniquely associated with fibroblast subsets that were enriched in *C. acnes*–infected skin (clusters 4 to 6) (Fig. 3E). Gene expression dot plots relating to fat cell differentiation GO terms are shown for infected versus noninfected samples and across all fibroblast clusters (fig. S3, A and B). Pseudotime analyses also revealed the presence of three separate lineages, with lineage 2 originating at cluster 9 and terminating with the proadipogenic and immunogenic clusters 4–6. Fibroblast clusters 4 and 5 shared similar differentiation trajectories across all three distinct lineages, which represent a transitional-like cellular state that has the potential to become a mature adipocyte population (Fig. 3F). Analysis of the top differentially expressed genes in *C. acnes*–enriched clusters 4 and 5 identified several antimicrobial response genes including complement factor H (*Cfh*) and the bacterial siderophore-binding lipocalin 2 (*Lcn2*) (Fig. 3G). Common among all three adipogenic clusters (4, 5, and 6) were genes involved in mediating immune-stromal cross-talk, including macrophage inflammatory protein-2 (*Mip-2/Cxcl2*), the chemokine *Cxcl9*, and *Il6* cytokine, which promote macrophage differentiation (29, 30).

Given the observed shifts in fibroblast transcriptional profiles during *C. acnes* infection, we speculated extensive cell-cell communication. To address this, we performed a ligand-receptor analysis using CellChat (31) to examine potential intercellular communication networks that might underlie the acne disease state. Nineteen signaling pathways were identified in acne, including pathways related to interleukin-1 (IL-1), tumor necrosis factor–α (TNFα), and CC chemokine ligands (CCL) (fig. S4A). The CCL signaling pathway network represented 11 ligand-receptor pairs across the 7 major cell types identified in the scRNA-seq dataset (fig. S4B). CellChat analysis also identified myeloid and fibroblast cells as dominant communication hubs, with CCL ligands being secreted by fibroblasts to myeloid cells (Fig. 3H). This result implies a separate but important role for reactive adipogenesis in communicating and regulating the host immune response toward *C. acnes* during acne development. Together, the scRNA-seq results highlighted specific fibroblast subpopulations that mount a response to *C. acnes* in mouse skin. These results are consistent with those obtained from the human acne samples, which demonstrate that reactive adipogenesis occurs in the perifollicular stroma in response to *C. acnes*. These observations support the conclusion that dermal fibroblasts play a role in the host immune response during acne development.

C. acnes enhances cathelicidin expression in cultured preadipocytes and is dependent on TLR2

To examine whether development of acne-like lesions in mice injected with *C. acnes* is dependent on reactive adipogenesis, mice were treated with bisphenol A diglycidyl ether (BADGE), a pharmacological inhibitor of peroxisome proliferator–activated receptor γ (PPARγ) and inhibitor of adipogenesis (10). Mice were treated with BADGE 1 day before *C. acnes* injection and throughout the duration of the experiment. Skin biopsies were collected on day 7, sectioned, and stained for lipid using BODIPY dye. As expected, mice treated with BADGE showed markedly less lipid accumulation in the dermal fibroblasts compared to nontreated mice (Fig. 4A). No change in BODIPY fluorescence was observed in sebaceous glands after BADGE treatment. Treatment with BADGE potently inhibited the capacity of *C. acnes* to induce lesions (Fig. 4B) and resulted in a striking decrease in bacterial colony-forming units (CFUs) recovered from the lesion (Fig. 4C). This result suggests that the growth of *C. acnes* benefits from the synthesis of lipid associated with reactive adipogenesis.

Expression of zinc finger protein 423 (ZFP423) is essential for committing fibroblasts to the preadipocyte lineage (10, 32). Adipogenesis progresses through the coordinated and temporal expression of several key transcriptional regulators, including *Cebpb* and *Cebpd*, which can induce *Camp* and *Pparg* expression (fig. S5A) (13, 33). Transcription of *Camp* is regulated by CCAAT/enhancer-binding protein β (C/EBPβ), which can bind to multiple available CCAAT sequences present on the *Camp* promoter. Additional putative regulatory sites on the *Camp* promoter include hypoxia response elements (HRE) that are regulated by hypoxia-inducible factor 1α (HIF-1α; fig. S5B) (13, 33–38). *Cebpa* is induced at later stages and acts in concert with *Pparg* to drive terminal adipocyte differentiation (39).
To better understand the mechanism by which *C. acnes* promotes reactive adipogenesis, sterile supernatant (SN) from *C. acnes* cultures was added to cultures of preadipocytes. SN increased *Cebpb* and *Camp* mRNA expression in both undifferentiated preadipocytes and differentiated immature adipocytes, and this effect was also observed during treatment with the Toll-like receptor (TLR) 2/6 ligand macrophage-activating lipopeptide-2 (MALP-2) (Fig. 4, D and E). Likewise, *Hifa* was increased in preadipocytes but not in immature adipocytes (fig. S5C). Increased cathelicidin protein was observed in preadipocytes treated with *C. acnes* SN (Fig. 4F). To better understand how *Camp* was induced by *C. acnes*, primary dermal fibroblasts were isolated from wild-type (WT) C57Bl6 mice and *Tlr2*$^{-/-}$ mice, and these mixed fibroblast primary cells were cultured with adipocyte differentiation medium or under nondifferentiating conditions. Both *Cebpb* and *Camp* were up-regulated in WT cells treated with MALP-2 or *C. acnes* SN, and this effect was reduced in cells lacking TLR2 (Fig. 4, G and H). In contrast, *Hif1a* expression was unaffected by the absence of TLR2 after stimulation with *C. acnes* SN (fig. S5D). This suggests that bacterial activation of TLR2 is a trigger for cathelicidin expression during reactive adipogenesis.

Retinoic acid increases preadipocyte cathelicidin and inhibits adipogenesis in response to *C. acnes*

Retinoids are highly effective in the treatment of acne (2, 40). Retinoids are believed to improve acne by acting on the capacity of the sebaceous gland to produce sebum (40,

41). To better understand the role of adipogenesis by dermal fibroblasts in acne formation, we next investigated how retinoic acid (RA) affected the mouse acne model. RA was administered for 3 days starting on day 3 after *C. acnes* challenge. Lesions were evaluated on day 6. Consistent with the benefits of retinoids in treating human acne, RA resulted in a marked decrease in the size or severity of *C. acnes* lesions on mice (Fig. 5, A and B). The resolution of *C. acnes* lesions corresponded with an increase in *Camp* mRNA expression (Fig. 5C) and a decrease in lipid staining in the dermis (Fig. 5D). Mice treated with RA also showed a decrease in neutrophils and neutrophil-associated cathelicidin protein (Fig. 5D). The increase in *Camp* in preadipocytes is consistent with a recent investigation that found that retinoids enhance cathelicidin expression (13) and suggested that RA may exert beneficial effects in acne by both increasing antimicrobial peptide expression and decreasing lipid accumulation in the dermis.

To evaluate the relative contribution of cathelicidin in the response to RA, we infected WT or *Camp* knockout mice ($Camp^{-/-}$) with *C. acnes* and treated both groups of mice with RA. $Camp^{-/-}$ mice lacking cathelicidin had larger lesions that did not resolve after RA treatment (Fig. 5E). RA treatment was associated with decreasing *Pref1* expression (Fig. 5F) but increasing *Hif1a* mRNA expression (fig. S6A), and this trend was unaffected in the $Camp^{-/-}$ mice. These observations confirmed the action of RA to inhibit adipocyte differentiation and the importance of *Camp* expression on lesion formation.

To directly examine whether *C. acnes* can influence the expression of *Camp* by preadipocytes exposed to retinoids, 3T3-L1 preadipocytes were cultured in the presence or absence of adipocyte differentiation medium with RA and sterile *C. acnes* SN. *Camp* expression was increased by *C. acnes* SN in both undifferentiated preadipocytes and immature adipocytes undergoing differentiation, but the greatest increase in expression of this antimicrobial peptide gene was seen when RA and *C. acnes* SN were combined (Fig. 5G).

These results led us to hypothesize that the beneficial action of retinoids in acne is linked to their capacity to influence the function of dermal fibroblasts. To further explore this concept, we examined the skin of patients before and after undergoing systemic treatment with isotretinoin, a retinoid that is highly effective for the treatment of severe acne. Because acne subjects treated with isotretinoin no longer had active lesions, we evaluated their response to skin wounding as a surrogate for the inflammatory lesion of acne. To do this, skin biopsies were first obtained from skin of the lower back, and the site of this initial biopsy was biopsied again 24 hours later (wound biopsy). Each subject had the same procedure both before and after concluding a full treatment course with isotretinoin. Comparison of the expression of cathelicidin in dermal preadipocytes of the wound biopsy before and after exposure to isotretinoin demonstrated an increase in the number of cells expressing cathelicidin after isotretinoin therapy (Fig. 5, H and I). In contrast, there was no apparent difference in cathelicidin expression in non-PREF1 cells, suggesting that preadipocytes are a cellular target during retinoid treatment.

Last, to validate that cathelicidin peptides from both humans and mice are active against *C. acnes*, synthetic peptides representing both the human and mouse cathelicidin gene

products were added to active cultures of *C. acnes*. Similar to prior observations with LL-37 (7), mouse CRAMP potently inhibited *C. acnes* growth, with an IC_{50} (median inhibitory concentration) of ~4 μM for human LL-37 and ~10 μM for mouse CRAMP (fig. S6B).

DISCUSSION

Acne vulgaris is an inflammatory disorder of the pilosebaceous gland of which *C. acnes* is a contributor (2, 42). Given the large psychosocial and economic impact of acne (1–4), numerous studies have sought to understand the pathophysiology of this disease. In this study, our findings have uncovered a response of human dermal fibroblasts in acne and in mice infected with *C. acnes*. The fibroblast response to *C. acnes* was at least partially dependent on TLR2, a pattern recognition receptor known to influence the inflammatory response (1, 2). The influence of fibroblasts on acne development appears to reflect a balance between host and microbe. Cells stimulated by *C. acnes* express cathelicidin, which has activity against *C. acnes*, whereas the induction of increased lipid synthesis appears to promote *C. acnes* growth. The effectiveness of retinoids in the treatment of acne may therefore be due to the capacity of retinoids to both inhibit lipid synthesis and increase the expression of cathelicidin. Together, these findings suggest that reactive adipogenesis in perifollicular dermal fibroblasts actively contributes to the pathophysiology of acne. This observation offers mechanistic insight into this common disease.

PREF1 is expressed primarily in preadipocytes (43), thus serving as one of defining hallmarks of adipogenesis (12). Upon initiation of reactive adipogenesis, preadipocyte differentiation is controlled by PREF1, and at the onset of differentiation, *Camp* expression is increased (10, 12). In the absence of bacterial infection, PREF1 and LL-37 are poorly expressed in the skin (10, 12, 14), but both are highly expressed within acne lesions and colocalize within the perifollicular region of the dermis. Crucially, LL-37 was not typically observed in the epidermis but instead localized to areas occupied by fibroblasts directly below the stratum basale as marked by positive K14 staining. Mice infected with *C. acnes* similarly exhibited elevated expression of both PREF1 and CRAMP and up-regulation of several other adipogenic factors within the dermis proximal to *C. acnes* lesions. scRNA-seq validated and advanced these observations and revealed that subpopulations of fibroblasts become activated during acne and express a fat cell differentiation program as well as genes associated with an antimicrobial and immune cell response. For example, *Lcn2* was found to be highly expressed in mouse fibroblast cluster 5, and is an antimicrobial peptide that, in addition to its role in binding and sequestering iron-scavenging bacterial siderophores to attenuate growth, has immunoregulatory functions affecting macrophage migration and phagocytosis (44, 45).

There are some limitations to the techniques used in this study. For example, *Camp* was not detected by scRNA-seq, potentially due to its smaller transcript size (2145 bases for *CAMP* versus 4383 bases for *LCN2*) (33). In addition, loss of intact mature adipocytes during tissue dissociation and single-cell retrieval limits the capacity to study these cells by scRNA-seq analysis. Adipocytes are highly sensitive to digestive enzymes due to their high lipid content, increased size, and buoyancy. This may also explain why certain genes such as *Pref1* were undetected, whereas some genes, such as *Camp*, were underrepresented

in our analyses (46). Nevertheless, qPCR and immunostaining of whole tissue confirmed expression of these genes, and our scRNA-seq validated previous findings from microarray on acne skin, namely, that *MMP1* and *MMP3* were highly expressed during acne and were associated with a single cluster (F1) in lesional acne (17). Despite the loss of adipocytes in the scRNA-seq dataset, we identified several gene clusters that were enriched for genes involved in fat cell differentiation. In *C. acnes*–infected skin, these clusters expressed gene sets that were immunogenic and consistent with a differentiation program into mature adipocytes.

While our data show that dermal fibroblasts are involved in acne, the factors that trigger their stimulation and differentiation are relatively unknown. We found that *C. acnes* injection into the dermis of mice was sufficient to induce an adipogenic profile in cells of the dermis. Previous studies have suggested that recognition of *C. acnes* by TLR2 is important for induction of an inflammatory response in acne (25, 47, 48). Similarly, knockout studies have shown that loss of TLR2 can attenuate the immune response to *C. acnes* (25, 49). Dermal adipocytes express high levels of TLR2 on their cell surface (50) and are naturally primed to recognize and respond to bacterial invasion. Additional studies have suggested that TLR2 signaling may enhance *Cebpb* expression and C/EBPβ translocation (51, 52). Induction of *Cebpb* expression is required to initiate adipogenesis and serves as an early adipogenic marker (34, 53), and the *Camp* promoter has multiple putative C/EBPβ-binding sites (33, 35–38). *Cebpb* and *Camp* were both up-regulated within 24 hours of *C. acnes* infection in vivo or exposure to *C. acnes* culture SN in vitro. We found that deletion of TLR2 in primary fibroblasts suppressed *Camp* and *Cebpb* expression when stimulated with *C. acnes* conditioned medium, supporting the contribution of TLR2 to acne and suggesting that adipocyte activation through C/EBPβ may also be an important signaling pathway in this disease. This is also consistent with observations that more inflammatory strains of *C. acnes* produce a toxin called Christie-Atkins-Munch-Petersen (CAMP) factor 1 that exhibits TLR2-binding activity (54). The prospect that distinct strains of *C. acnes* may differ in their capacity to trigger reactive adipogenesis is an area of active investigation.

Retinoids are effective therapeutics in the treatment of acne. Their mechanism of action has been attributed to suppressive activity on the sebaceous gland or keratinocytes (3, 40, 41, 55). Isotretinoin (13-*cis* RA) has also been shown to down-regulate TLR2 signaling in monocytes and reduce overall inflammation in acne (48). This therapeutic activity of RA was modeled in *C. acnes*–infected SKH-1 hairless mice, resulting in reduced lesion size and disease severity score. *C. acnes*–induced lesions were less pronounced in C57BL/6 mice, but infected *Camp*$^{-/-}$ mice in this strain background developed large lesions that did not improve after treatment with RA. We found that acne patients treated with isotretinoin showed greater cathelicidin expression in dermal fibroblasts. This suggests that RA may have additional therapeutic effects by also increasing cathelicidin expression. This is consistent with previous studies that have found that retinoids enhance *Hif1a* and *Camp* expression (13). It is not clear whether the effect observed in *Camp*$^{-/-}$ mice was due to loss of cathelicidin from neutrophils, fibroblasts, or other cells. However, cathelicidin in neutrophils is not typically inducible since it is produced by neutrophils while they mature in the bone marrow (10, 56) and not likely a target of RA. Furthermore, given the abundance of cathelicidin expressed in fibroblasts, and the large decrease in neutrophils seen in mice after

RA treatment, it is probable that the loss of expression of *Camp* from fibroblasts contributed to the increased disease observed in *Camp*$^{-/-}$ mice.

Therefore, it is attractive to speculate that RA benefits acne subjects because it can both induce cathelicidin and decrease lipid synthesis in the dermal preadipocyte. These observations reveal an unexpected and important role for perifollicular fibroblasts in the development and resolution of acne.

MATERIALS AND METHODS

Study design

The aim of this study was to understand the role of dermal fibroblasts in acne. After informed consent, skin biopsies were performed on acne lesions and uninvolved skin from the back of study participants. Biopsies were analyzed by scRNA-seq, immunostaining, and qPCR for select genes of interest. To model acne-like lesions in mice, *C. acnes* was intradermally injected into mouse back skin and a transcriptional and histological analysis was performed that was similar to analysis used for human skin. *C. acnes* sterile conditioned SN was added in cell cultures of preadipocytes and primary fibroblasts (with or without *Tlr2*) to study the capacity to trigger fibroblast responses in vitro that model the observed response in human and mouse skin. Chemical treatment by BADGE (PPARγ inhibitor) and RA was evaluated to test the role of adipogenesis in development of acne-like lesions in mice and *Camp* knockout mice used to test the dependence on cathelicidin. Skin biopsies were also evaluated from acne patients before and after treatment with 13-*cis* RA (isotretinoin).

Antibodies, chemicals, and reagents

3-Isobutyl-1-methylxanthine (IBMX), dexamethasone, indomethacin, recombinant human insulin, squalene, and all-*trans* RA were purchased from Sigma-Aldrich (St. Louis, MO). MALP-2 was purchased from Enzo Life Sciences. Rabbit anti-CRAMP and rabbit anti–LL-37 antibodies were made in our laboratory as previously described (57). BODIPY was purchased from Thermo Fisher Scientific. Rabbit anti-PREF1 (DLK1) antibody was purchased from GeneTex (GTX60309). Synthetic LL-37 was purchased from Genemed Synthesis. Synthetic CRAMP peptide was purchased from Sigma-Genosys. BADGE was purchased from Santa Cruz Biotechnology (Santa Cruz, CA) (sc202487). Anti-neutrophil marker antibody was purchased from Santa Cruz Biotechnology (sc71674).

Bacterial strains and bacterial culture

C. acnes laboratory strains [61.CaUCSD and 2.CaUCSD (phylotype IA1)] were grown on Brucella blood agar plates and grown for 5 days at 37°C under anaerobic conditions. Single-colony isolates were resuspended in 3 ml of reinforced clostridial medium (RCM) and grown for 5 to 7 days at 37°C under anaerobic conditions. For in vivo and antimicrobial experiments, bacteria were pelleted, resuspended, and diluted in fresh RCM to approximately 1×10^7 CFU. To examine the effects of *C. acnes* in vitro, SNs were filtered through a 0.22-μm filter. Sterile filtrate was then added to cultured cells.

Human skin sample collection

Fresh adult human skin biopsies, from the back of healthy donors (age 18 to 50), were collected from the Dermatology Clinic, University of California, San Diego (UCSD) and from the Dermatology Clinic, University of Michigan, Ann Arbor. Sample acquisitions were approved and regulated by the UCSD Institutional Review Board (IRB; reference number 140144) and University of Michigan IRB (HUM00174864). Experiments involving human subjects treated with isotretinoin (Accutane) were carried out according to IRB protocol approved by UCSD (#171939). Two patients (age 22 and 27) with moderate-to-severe acne were recruited, and an active lesion was biopsied before isotretinoin treatment. Patients received isotretinoin for 4.5 to 5.5 months and received a biopsy from the back skin site of a former lesional area at the conclusion of treatment. Twenty-four hours later, patients then received a second biopsy (wound biopsy) proximal to the first biopsy. Biopsies were immediately embedded in Tissue-Tek optimal cutting temperature (OCT) compound for sectioning and staining. The informed consent was obtained from all subjects before skin biopsies. Upon collection, these samples were directly OCT-embedded for histological or immunofluorescent analyses or enzymatically digested and processed into single-cell suspension for scRNA-seq, as previously described (58).

Animals and animal care

All animal experiments were approved by the UCSD Institutional Animal Care and Use Committee. SKH-1 hairless mice and WT, *Tlr2*$^{-/-}$, and *Camp*$^{-/-}$ C57/Bl6 mice were originally purchased from The Jackson Laboratory, bred, and maintained in animal facility of UCSD. Animals in all experimental models were age- and sex-matched.

Mouse model of *C. acnes* skin infection

To promote the formation of acne-like lesions in mice, 100 μl of squalene was topically applied to the backs of age-matched (8 to 10 weeks) SKH-1 mice 24 hours before infection and every 24 hours thereafter throughout the duration of the experiment according to (27). Mice were intradermally injected with approximately 1×10^7 CFU of *C. acnes* or control (PBS or RCM). For RA experiments, mice were distally administered one subcutaneous dose of RA (10 mg/kg) or vehicle [dimethyl sulfoxide (DMSO)] dissolved in olive oil on days 3, 4, and 5. Mice treated with BADGE (30 mg/kg) were injected intraperitoneally daily starting 1 day before infection or vehicle control (10% DMSO in PBS). Images of mouse back skin were taken with a Panasonic Lumix TS30 digital camera, and *C. acnes*–infected skin lesions were clinically evaluated with an investigator assessment of lesion severity ranging from 0 (no lesion detected) to 4 (severe). On indicated days, mice were sacrificed and an 8-mm skin biopsy of the infected region was performed. Skin samples were then homogenized in PureLink Lysis Buffer with 2-mm zirconia beads in a mini-bead beater (BioSpec, Bartlesville, OK) for RNA extraction or directly embedded in OCT for tissue sectioning and histology.

Histology and immunohistochemistry

Tissue biopsies were directly embedded in OCT compound and sectioned 10–20 μm thick at −20°C using a Leica CM1860 cryostat. BODIPY solution was used to visualize lipid

droplets. Frozen tissue sections were stained with primary antibodies overnight at 4°C, secondary antibodies for 1 hour at room temperature, and nuclei were counterstained with 4′,6-diamidino-2-phenylindole (DAPI). All images were taken with an Olympus BX41 microscope.

Confocal microscopy and image quantification

Tissue sections were imaged on a Nikon A1R microscope, and images were processed using NIS Elements AR Analysis software (version 5.21.01). Images were first subjected to denoise using the NIS.ai tool. Quantification was done by using analysis explorer and by adding Combined Layers in the Analysis Palette feature, with the application of the selected binary operations "AND" to include areas of overlap between that of cy3 (CAMP-positive) and fluorescein isothiocyanate (FITC; PREF1-positive) channels and cy3 "SUB" FITC to include areas of cy3 (CAMP-positive) that do not overlap with FITC (PREF1). Manual thresholding was performed, and values were kept consistent for all images that were quantified. The application was run, and the fluorescence values were obtained by selecting the "automated measurement results" tool. The integrated intensity values were generated for the combined layers, and the results were exported to Excel for graph plotting.

Cell culture

3T3-L1 primary mouse preadipocytes were purchased from the American Type Culture Collection (CL-173). Neonatal primary dermal fibroblasts (WT and *Tlr2*$^{-/-}$) were isolated by our laboratory as previously described (59). Cells were grown in Dulbecco's Modified Eagle Medium (DMEM) supplemented with 10% fetal bovine serum (FBS), Glutamax, and antibiotic-antimycotic (Thermo Fisher Scientific) in a humidified incubator at 5% CO_2 and 37°C under sterile conditions. To induce differentiation, 2-day postconfluent cells were switched to adipocyte differentiation medium containing 2 μM dexamethasone, 250 μM IBMX, 200 μM indomethacin, and recombinant human insulin (10 μg/ml). The 2.5% (v/v) sterile *C. acnes* SN was simultaneously added to postconfluent cells. To examine the effects of retinoids, 1 μM RA or vehicle (ethanol) was added to cell culture medium on day 0.

RNA isolation, cDNA synthesis, and reverse transcription qPCR analysis

Cultured cells and isolated tissues were directly lysed using PureLink Lysis Buffer (Ambion/Life Technologies) and RNA were isolated using a PureLink Isolation kit. For RNA extraction from human acne tissue sections, a total of 30 sections were collected per biopsy and combined for RNA extraction using TRIzol (Thermo Fisher Scientific). Up to 1 μg of RNA was reverse-transcribed to complementary DNA (cDNA) using a Verso cDNA synthesis kit (Fisher Scientific). Quantitative real-time PCR was performed with the CFX96 Real-Time System (Bio-Rad) using SYBR Green Mix (Bimake, Houston, TX). The housekeeping gene *Tbp* (TATA-binding box protein) or *Gapdh* was used to normalize gene expression in samples. Specific primer sequences are shown in table S1.

Single-cell analysis of human and mouse skin

Samples were collected in accordance with protocols approved by the IRB at the University of California, Los Angeles. Acne donors were recruited from the University

of California, Los Angeles, and all patients provided written informed consent. Patients were excluded from the study if they had been using acne medication, hormone medication, or hormone-related implants in 3 months before sampling. Skin samples were collected from 3-mm punch biopsies in the back and processed as previously described (60). The recovered viable single cells were loaded into the Chromium instrument (10X Genomics) according to the manufacturer's protocol and analyzed using Seurat (19, 20). All animal experiments were approved by the UCSD Institutional Animal Care and Use Committee (#S09074). For scRNA-seq analysis of mouse skin, the upper back skin of SKH-1 mice was intradermally infected with 1×10^7 CFU of *C. acnes* or RCM control for 3 days. Skin samples were collected from 6-mm punch biopsies and immediately placed on ice. In total, three biopsies were pooled per condition (infected or noninfected) for single-cell generation. Single-cell suspensions were generated by cutting skin into small pieces using a scalpel followed by digestion in Hanks' balanced salt solution (Thermo Fisher Scientific, #14175095) supplemented with bovine serum albumin (20 mg/ml), 1× antibiotic-antimycotic (Thermo Fisher Scientific, #15240062), deoxyribonuclease I (50 U/ml; Sigma-Aldrich, #04716728001), Liberase (0.1 mg/ml; Sigma-Aldrich, #05401020001), 20 mM Hepes (Thermo Fisher Scientific, #15630080), 2 mM sodium pyruvate (Thermo Fisher Scientific, #11360070), and collagenase type IV (1 mg/ml; Thermo Fisher Scientific, #17104019). Tissue dissociation was carried out by a 2-hour ice-cold incubation in the digestion buffer followed by 45-min incubation at 37°C shaking at 200 rpm. Enzymatic dissociation was terminated by addition of 5 mM EDTA and 10% FBS. Digests were filtered twice through a 40-μm filter and then incubated in red blood cell lysis buffer followed by removal of dead cell using the MACS Dead Cell Removal Kit (Miltenyi Biotec) for downstream applications in 10X Genomics Chromium platform.

The 10X Genomics Cell Ranger version 3.0.1 software pipeline with default parameters was used to perform sample demultiplexing, barcode processing, alignment to the mm10 reference genome, and single-cell gene counting. Data were further filtered, processed, and analyzed using the Seurat R toolkit version 3 (61, 62). Filtering of initial data involved selecting cells with >100 features and <10% mitochondrial genes. Data were normalized using the NormalizeData() function with parameters normalization.method = 'LogNormalize' and scale.factor = 10000. Variable genes were identified with the FindVariableFeatures() function with parameters selection. method = 'vst'. Data were scaled with the ScaleData() function with default parameters. Principal components (PCs) were calculated from these variable genes using the function RunPCA(), and the top 20 PCs were used for downstream analysis. Clusters were identified using the FindNeighbors() and then FindClusters() function with arguments resolution = 0.5. Nonlinear dimensionality reduction and visualization were performed with tSNE using the RunTSNE() function, and UMAP (63) using the RunUMAP() function. Marker genes for each cluster were determined using the FindAllMarkers() function with parameters only.pos = TRUE, min.pct = 0.25, and thresh.use = 0.25. Clusters were assigned to cell types "Fibroblast," "Keratinocyte," "Myeloid," "Lymphoid," "Endothelial," and "Melanocyte" based on marker genes. Six of the original 24 clusters were annotated as fibroblasts and underwent additional quality control. In brief, a new Seurat object was generated using only the cells in these clusters with their corresponding raw counts, followed by normalization, scaling, clustering, and

dimensionality reduction as described above, resulting in 15 fibroblast clusters. Clusters with high expression of leukocyte marker genes and cell cycle genes were excluded, and a final Seurat object was created from the remaining cells and their raw counts with a final iteration of normalization, scaling, clustering, and dimensionality reduction. Cluster marker genes were identified on the finalized 10 clusters with FindAllMarkers() with parameters only.pos = TRUE and thresh.use = 0.4054651 (corresponding to 1.5 fold change). GO analysis was performed on marker genes using the "clusterProfiler" R package with default parameters (64). Cell lineage and pseudotime inference were performed using the Slingshot R package (23). The Seurat object was transformed into a SingleCellExperiment object, and Slingshot trajectory analysis was performed using Seurat clustering information and UMAP dimensionality reduction. We used the standard workflow of the recently developed package CellChat to perform cellular communication analysis and visualization of our scRNA-seq data (32).

Antimicrobial assay

C. acnes was cultured in RCM at 37°C in an anaerobic pouch (Oxoid, AnaeroGen) until mid-log phase. The bacteria were then inoculated at a concentration of 5×10^5 CFU/ml into a 96-well round-bottom plate containing a serial dilution of human (LL-37) or mouse cathelicidin peptide in EpiLife medium (as a source of calcium and magnesium) that was supplemented with RCM to support *C. acnes* growth. After 48 hours of anaerobic growth at 37°C, the optical density was measured at 600 nm on a microplate reader.

Statistical analysis

Experiments conducted were performed in triplicate with at least three technical replicates. Statistical significance was calculated using a one-way analysis of variance (ANOVA) with Tukey's multiple comparison test and Student's two-tailed *t* test, where $*P < 0.05$, $**P < 0.01$, $***P < 0.001$, and $****P < 0.0001$, as indicated in figure legends.

Study approval

All animal experiments were approved by the UCSD Institutional Animal Care and Use Committee (#S09074). For human studies, all sample acquisitions were approved and regulated by the UCSD IRB (reference number 140144) or by the University of Michigan IRB (HUM00174864). Informed consent was obtained from all subjects before skin biopsies (IRB #171939).

Supplementary Material

Refer to Web version on PubMed Central for supplementary material.

Acknowledgments:

We thank the Cancer Center Microscopy core for providing microscopes and imaging software. The Cancer Center Microscopy core is supported by the UCSD Specialized Cancer Center Support Grant (NCI) P30 2P30CA023100.

Funding:

This study was supported by NIH grants R37AI052453 (R.L.G.), R01AR069653 (R.L.G.), R01AR074302 (R.L.G. and R.L.M.), P30 AR075043 (J.E.G.), and T32 (K.J.C.) and an American Acne and Rosacea Society (AARS) clinical research grant (A.M.O.).

Data and materials availability:

All data associated with this study are present in the paper or the Supplementary Materials. The human acne scRNA-seq data are available at the Gene Expression Omnibus (GEO) under accession no. GSE175817, and the mouse scRNA-seq data can be found under accession no. GSE193584. Materials will be made available by contacting R.L.G. and completion of a material transfer agreement.

REFERENCES AND NOTES

1. Sanford JA, O'Neill AM, Zouboulis CC, Gallo RL, Short-chain fatty acids from Cutibacterium acnesActivate both a canonical and epigenetic inflammatory response in human sebocytes. J. Immunol. 202, 1767–1776 (2019). [PubMed: 30737272]
2. O'Neill AM, Gallo RL, Host-microbiome interactions and recent progress into understanding the biology of acne vulgaris. Microbiome 6, 177 (2018). [PubMed: 30285861]
3. Chen B, Li P, Li J, Chen J, Putative genes and pathways involved in the acne treatment of isotretinoin via microarray data analyses. Biomed. Res. Int. 2020, 1–14 (2020).
4. Laughlin JM, Watterson S, Layton AM, Bjourson AJ, Barnard E, Dowell AM, Propionibacterium acnes and acne vulgaris: New insights from the integration of population genetic, multi-omic, biochemical and host-microbe studies. Microorganisms 7, 128 (2019). [PubMed: 31086023]
5. Kovács D, Lovászi M, Póliska S, Oláh A, Bíró T, Veres I, Zouboulis CC, Ståhle M, Rühl R, Remenyik É, Törőcsik D, Sebocytes differentially express and secrete adipokines. Exp. Dermatol. 25, 194–199 (2016). [PubMed: 26476096]
6. Sanford JA, Zhang LJ, Williams MR, Gangoiti JA, Huang CM, Gallo RL, Inhibition of HDAC8 and HDAC9 by microbial short-chain fatty acids breaks immune tolerance of the epidermis to TLR ligands. Sci. Immunol 1, eaah4609 (2016). [PubMed: 28783689]
7. Lee DY, Yamasaki K, Rudsil J, Zouboulis CC, Park GT, Yang JM, Gallo RL, Sebocytes express functional cathelicidin antimicrobial peptides and can act to kill propionibacterium acnes. J. Invest. Dermatol. 128, 1863–1866 (2008). [PubMed: 18200058]
8. Sanford JA, Gallo RL, Functions of the skin microbiota in health and disease. Semin. Immunol. 25, 370–377 (2013). [PubMed: 24268438]
9. Chen SX, Zhang LJ, Gallo RL, Dermal white adipose tissue: A newly recognized layer of skin innate defense. J. Invest. Dermatol. 139, 1002–1009 (2019). [PubMed: 30879642]
10. Zhang LJ, Guerrero-Juarez CF, Hata T, Bapat SP, Ramos R, Plikus MV, Gallo RL, Innate immunity. Dermal adipocytes protect against invasive Staphylococcus aureus skin infection. Science 347, 67–71 (2015). [PubMed: 25554785]
11. Zhang Z, Shao M, Hepler C, Zi Z, Zhao S, An YA, Zhu Y, Ghaben AL, Wang MY, Li N, Onodera T, Joffin N, Crewe C, Zhu Q, Vishvanath L, Kumar A, Xing C, Wang QA, Gautron L, Deng Y, Gordillo R, Kruglikov I, Kusminski CM, Gupta RK, Scherer PE, Dermal adipose tissue has high plasticity and undergoes reversible dedifferentiation in mice. J. Clin. Invest. 129, 5327–5342 (2019). [PubMed: 31503545]
12. Zhang L-J, Chen SX, Guerrero-Juarez CF, Li F, Tong Y, Liang Y, Liggins M, Chen X, Chen H, Li M, Hata T, Zheng Y, Plikus MV, Gallo RL, Age-related loss of innate immune antimicrobial function of dermal fat is mediated by transforming growth factor beta. Immunity 50, 121–136 e125 (2019). [PubMed: 30594464]
13. Liggins MC, Li F, Zhang LJ, Dokoshi T, Gallo RL, Retinoids enhance the expression of cathelicidin antimicrobial peptide during reactive dermal adipogenesis. J. Immunol. 203, 1589–1597 (2019). [PubMed: 31420464]

14. Dokoshi T, Zhang LJ, Nakatsuji T, Adase CA, Sanford JA, Paladini RD, Tanaka H, Fujiya M, Gallo RL, Hyaluronidase inhibits reactive adipogenesis and inflammation of colon and skin. JCI Insight 3, e123072 (2018). [PubMed: 30385720]

15. Dokoshi T, Zhang L-J, Li F, Nakatsuji T, Butcher A, Yoshida H, Shimoda M, Okada Y, Gallo RL, Hyaluronan degradation by cemip regulates host defense against staphylococcus aureus skin infection. Cell Rep. 30, 61–68.e64 (2020). [PubMed: 31914398]

16. Palhinha L, Liechocki S, Hottz ED, da Silva Pereira JA, de Almeida CJ, Moraes-Vieira PMM, Bozza PT, Maya-Monteiro CM, Leptin induces proadipogenic and proinflammatory signaling in adipocytes. Front. Endocrinol. 10, 841 (2019).

17. Trivedi NR, Gilliland KL, Zhao W, Liu W, Thiboutot DM, Gene array expression profiling in acne lesions reveals marked upregulation of genes involved in inflammation and matrix remodeling. J. Invest. Dermatol. 126, 1071–1079 (2006). [PubMed: 16528362]

18. Kang S, Cho S, Chung JH, Hammerberg C, Fisher GJ, Voorhees JJ, Inflammation and extracellular matrix degradation mediated by activated transcription factors nuclear factor-kappaB and activator protein-1 in inflammatory acne lesions in vivo. Am. J. Pathol. 166, 1691–1699 (2005). [PubMed: 15920154]

19. Zhang LJ, Guerrero-Juarez CF, Chen SX, Zhang X, Yin M, Li F, Wu S, Chen J, Li M, Liu Y, Jiang SIB, Hata T, Plikus MV, Gallo RL, Diet-induced obesity promotes infection by impairment of the innate antimicrobial defense function of dermal adipocyte progenitors. Sci. Transl. Med. 13, eabb5280 (2021). [PubMed: 33472955]

20. Hughes RM, Simons BW, Khan H, Miller R, Kugler V, Torquato S, Theodros D, Haffner MC, Lotan T, Huang J, Davicioni E, An SS, Riddle RC, Thorek DLJ, Garraway IP, Fertig EJ, Isaacs JT, Brennen WN, Park BH, Hurley PJ, Asporin restricts mesenchymal stromal cell differentiation, alters the tumor microenvironment, and drives metastatic progression. Cancer Res. 79, 3636–3650 (2019). [PubMed: 31123087]

21. Maris P, Blomme A, Palacios AP, Costanza B, Bellahcène A, Bianchi E, Gofflot S, Drion P, Trombino GE, di Valentin E, Cusumano PG, Maweja S, Jerusalem G, Delvenne P, Lifrange E, Castronovo V, Turtoi A, Asporin is a fibroblast-derived TGF-β1 inhibitor and a tumor suppressor associated with good prognosis in breast cancer. PLOS Med. 12, e1001871 (2015). [PubMed: 26327350]

22. Park SW, Huang WH, Persaud SD, Wei LN, RIP140 in thyroid hormone-repression and chromatin remodeling of Crabp1 gene during adipocyte differentiation. Nucleic Acids Res. 37, 7085–7094 (2009). [PubMed: 19778926]

23. Street K, Risso D, Fletcher RB, Das D, Ngai J, Yosef N, Purdom E, Dudoit S, Slingshot: Cell lineage and pseudotime inference for single-cell transcriptomics. BMC Genomics 19, 477 (2018). [PubMed: 29914354]

24. Jugeau S, Tenaud I, Knol AC, Jarrousse V, Quereux G, Khammari A, Dreno B, Induction of toll-like receptors by Propionibacterium acnes. Br. J. Dermatol. 153, 1105–1113 (2005). [PubMed: 16307644]

25. Kim J, Ochoa MT, Krutzik SR, Takeuchi O, Uematsu S, Legaspi AJ, Brightbill HD, Holland D, Cunliffe WJ, Akira S, Sieling PA, Godowski PJ, Modlin RL, Activation of toll-like receptor 2 in acne triggers inflammatory cytokine responses. J. Immunol. 169, 1535–1541 (2002). [PubMed: 12133981]

26. Vowels BR, Yang S, Leyden JJ, Induction of proinflammatory cytokines by a soluble factor of Propionibacterium acnes: Implications for chronic inflammatory acne. Infect. Immun. 63, 3158–3165 (1995). [PubMed: 7542639]

27. Kolar SL, Tsai CM, Torres J, Fan X, Li H, Liu GY, Propionibacterium acnes-induced immunopathology correlates with health and disease association. JCI Insight 4, e124687 (2019). [PubMed: 30843879]

28. Nikkari T, Comparative chemistry of sebum. J. Invest. Dermatol. 62, 257–267 (1974). [PubMed: 4206501]

29. Mauer J, Chaurasia B, Goldau J, Vogt MC, Ruud J, Nguyen KD, Theurich S, Hausen AC, Schmitz J, Brönneke HS, Estevez E, Allen TL, Mesaros A, Partridge L, Febbraio MA, Chawla A, Wunderlich FT, Brüning JC, Signaling by IL-6 promotes alternative activation of macrophages to

limit endotoxemia and obesity-associated resistance to insulin. Nat. Immunol. 15, 423–430 (2014). [PubMed: 24681566]

30. Tokunaga R, Zhang W, Naseem M, Puccini A, Berger MD, Soni S, McSkane M, Baba H, Lenz HJ, CXCL9, CXCL10, CXCL11/CXCR3 axis for immune activation—A target for novel cancer therapy. Cancer Treat. Rev. 63, 40–47 (2018). [PubMed: 29207310]
31. Jin S, Guerrero-Juarez CF, Zhang L, Chang I, Ramos R, Kuan CH, Myung P, Plikus MV, Nie Q, Inference and analysis of cell-cell communication using CellChat. Nat. Commun. 12, 1088 (2021). [PubMed: 33597522]
32. Gupta RK, Arany Z, Seale P, Mepani RJ, Ye L, Conroe HM, Roby YA, Kulaga H, Reed RR, Spiegelman BM, Transcriptional control of preadipocyte determination by Zfp423. Nature 464, 619–623 (2010). [PubMed: 20200519]
33. Elloumi HZ, Holland SM, Complex regulation of human cathelicidin gene expression: Novel splice variants and 5'UTR negative regulatory element. Mol. Immunol. 45, 204–217 (2008). [PubMed: 17709140]
34. Darlington GJ, Ross SE, MacDougald OA, The role of C/EBP genes in adipocyte differentiation. J. Biol. Chem. 273, 30057–30060 (1998). [PubMed: 9804754]
35. Wu H, Zhang G, Minton JE, Ross CR, Blecha F, Regulation of cathelicidin gene expression: Induction by lipopolysaccharide, interleukin-6, retinoic acid, and Salmonella enterica serovar typhimurium infection. Infect. Immun. 68, 5552–5558 (2000). [PubMed: 10992453]
36. Pestonjamasp VK, Huttner KH, Gallo RL, Processing site and gene structure for the murine antimicrobial peptide CRAMP. Peptides 22, 1643–1650 (2001). [PubMed: 11587792]
37. Miraglia E, Nylén F, Johansson K, Arnér E, Cebula M, Farmand S, Ottosson H, Strömberg R, Gudmundsson GH, Agerberth B, Bergman P, Entinostat up-regulates the CAMP gene encoding LL-37 via activation of STAT3 and HIF-1α transcription factors. Sci. Rep. 6, 33274 (2016). [PubMed: 27633343]
38. Gombart AF, Borregaard N, Koeffler HP, Human cathelicidin antimicrobial peptide (CAMP) gene is a direct target of the vitamin D receptor and is strongly up-regulated in myeloid cells by 1,25-dihydroxyvitamin D3. FASEB J. 19, 1067–1077 (2005). [PubMed: 15985530]
39. Lefterova MI, Zhang Y, Steger DJ, Schupp M, Schug J, Cristancho A, Feng D, Zhuo D, Stoeckert CJ Jr., Liu XS, Lazar MA, PPARgamma and C/EBP factors orchestrate adipocyte biology via adjacent binding on a genome-wide scale. Genes Dev. 22, 2941–2952 (2008). [PubMed: 18981473]
40. Chivot M, Retinoid therapy for acne. A comparative review. Am. J. Clin. Dermatol. 6, 13–19 (2005). [PubMed: 15675886]
41. Nelson AM, Zhao W, Gilliland KL, Zaenglein AL, Liu W, Thiboutot DM, Neutrophil gelatinase-associated lipocalin mediates 13-cis retinoic acid-induced apoptosis of human sebaceous gland cells. J. Clin. Invest. 118, 1468–1478 (2008). [PubMed: 18317594]
42. Dreno B, What is new in the pathophysiology of acne, an overview. J. Eur. Acad. Dermatol. 31, 8–12 (2017).
43. Wang Y, Kim KA, Kim JH, Sul HS, Pref-1, a preadipocyte secreted factor that inhibits adipogenesis. J. Nutr. 136, 2953–2956 (2006). [PubMed: 17116701]
44. Berger T, Togawa A, Duncan GS, Elia AJ, You-ten A, Wakeham A, Fong HEH, Cheung CC, Mak TW, Lipocalin 2-deficient mice exhibit increased sensitivity to Escherichia coli infection but not to ischemia-reperfusion injury. Proc. Natl. Acad. Sci. U.S.A. 103, 1834–1839 (2006). [PubMed: 16446425]
45. Wang Q, Li S, Tang X, Liang L, Wang F, du H, Lipocalin 2 protects against escherichia coli infection by modulating neutrophil and macrophage function. Front. Immunol. 10, 2594 (2019). [PubMed: 31781104]
46. Deutsch A, Feng D, Pessin JE, Shinoda K, The impact of single-cell genomics on adipose tissue research. Int. J. Mol. Sci. 21, 4773 (2020). [PubMed: 32635651]
47. Zhang B, Choi YM, Lee J, An IS, Li L, He C, Dong Y, Bae S, Meng H, Toll-like receptor 2 plays a critical role in pathogenesis of acne vulgaris. Biomed. Dermatol. 3, 4 (2019).

48. Dispenza MC, Wolpert EB, Gilliland KL, Dai JP, Cong Z, Nelson AM, Thiboutot DM, Systemic isotretinoin therapy normalizes exaggerated TLR-2-mediated innate immune responses in acne patients. J. Invest. Dermatol. 132, 2198–2205 (2012). [PubMed: 22513780]
49. Kim J, Review of the innate immune response in acne vulgaris: Activation of Toll-like receptor 2 in acne triggers inflammatory cytokine responses. Dermatology 211, 193–198 (2005). [PubMed: 16205063]
50. Bès-Houtmann S, Roche R, Hoareau L, Gonthier M-P, Festy F, Caillens H, Gasque P, d'Hellencourt CL, Cesari M, Presence of functional TLR2 and TLR4 on human adipocytes. Histochem. Cell Biol. 127, 131–137 (2007). [PubMed: 16988837]
51. Hu J, Roy SK, Shapiro PS, Rodig SR, Reddy SPM, Platanias LC, Schreiber RD, Kalvakolanu DV, ERK1 and ERK2 activate CCAAAT/enhancer-binding protein-beta-dependent gene transcription in response to interferon-gamma. J. Biol. Chem. 276, 287–297 (2001). [PubMed: 10995751]
52. Wang JE, Dahle MK, McDonald M, Foster SJ, Aasen AO, Thiemermann C, Peptidoglycan and lipoteichoic acid in gram-positive bacterial sepsis: Receptors, signal transduction, biological effects, and synergism. Shock 20, 402–414 (2003). [PubMed: 14560103]
53. Lefterova MI, Haakonsson AK, Lazar MA, Mandrup S, PPARγ and the global map of adipogenesis and beyond. Trends Endocrinol. Metab. 25, 293–302 (2014). [PubMed: 24793638]
54. Lheure C, Grange PA, Ollagnier G, Morand P, Désiré N, Sayon S, Corvec S, Raingeaud J, Marcelin AG, Calvez V, Khammari A, Batteux F, Dréno B, Dupin N, TLR-2 recognizes propionibacterium acnes camp factor 1 from highly inflammatory strains. PLOS One 11, e0167237 (2016). [PubMed: 27902761]
55. Roeder A, Schaller M, Schafer-Korting M, Korting HC, Tazarotene: Therapeutic strategies in the treatment of psoriasis, acne and photoaging. Skin Pharmacol. Physiol. 17, 111–118 (2004). [PubMed: 15087589]
56. Gallo RL, Kim KJ, Bernfield M, Kozak CA, Zanetti M, Merluzzi L, Gennaro R, Identification of CRAMP, a cathelin-related antimicrobial peptide expressed in the embryonic and adult mouse. J. Biol. Chem. 272, 13088–13093 (1997). [PubMed: 9148921]
57. Dorschner RA, Pestonjamasp VK, Tamakuwala S, Ohtake T, Rudisill J, Nizet V, Agerberth B, Gudmundsson GH, Gallo RL, Cutaneous injury induces the release of cathelicidin anti-microbial peptides active against group A Streptococcus. J. Invest. Dermatol. 117, 91–97 (2001). [PubMed: 11442754]
58. Gudjonsson JE, Tsoi LC, Ma F, Billi AC, van Straalen KR, Vossen ARJV, van der Zee HH, Harms PW, Wasikowski R, Yee CM, Rizvi SM, Xing X, Xing E, Plazyo O, Zeng C, Patrick MT, Lowe MM, Burney RE, Kozlow JH, Cherry-Bukowiec JR, Jiang Y, Kirma J, Weidinger S, Cushing KC, Rosenblum MD, Berthier C, MacLeod AS, Voorhees JJ, Wen F, Kahlenberg JM, Maverakis E, Modlin RL, Prens EP, Contribution of plasma cells and B cells to hidradenitis suppurativa pathogenesis. JCI Insight 5, e139930 (2020). [PubMed: 32853177]
59. Vu BG, Gourronc FA, Bernlohr DA, Schlievert PM, Klingelhutz AJ, Staphylococcal superantigens stimulate immortalized human adipocytes to produce chemokines. PLOS ONE 8, e77988 (2013). [PubMed: 24205055]
60. Hildreth AD, Ma F, Wong YY, Sun R, Pellegrini M, O'Sullivan TE, Single-cell sequencing of human white adipose tissue identifies new cell states in health and obesity. Nat. Immunol. 22, 639–653 (2021). [PubMed: 33907320]
61. Butler A, Hoffman P, Smibert P, Papalexi E, Satija R, Integrating single-cell transcriptomic data across different conditions, technologies, and species. Nat. Biotechnol. 36, 411–420 (2018). [PubMed: 29608179]
62. Stuart T, Butler A, Hoffman P, Hafemeister C, Papalexi E, Mauck III WM, Hao Y, Stoeckius M, Smibert P, Satija R, Comprehensive integration of single-cell data. Cell 177, 1888–1902.e1821 (2019). [PubMed: 31178118]
63. Becht E, McInnes L, Healy J, Dutertre C-A, Kwok IWH, Ng LG, Ginhoux F, Newell EW, Dimensionality reduction for visualizing single-cell data using UMAP. Nat. Biotechnol. 37, 38–44 (2019).
64. Yu G, Wang LG, Han Y, He QY, clusterProfiler: An R package for comparing biological themes among gene clusters. OMICS 16, 284–287 (2012). [PubMed: 22455463]

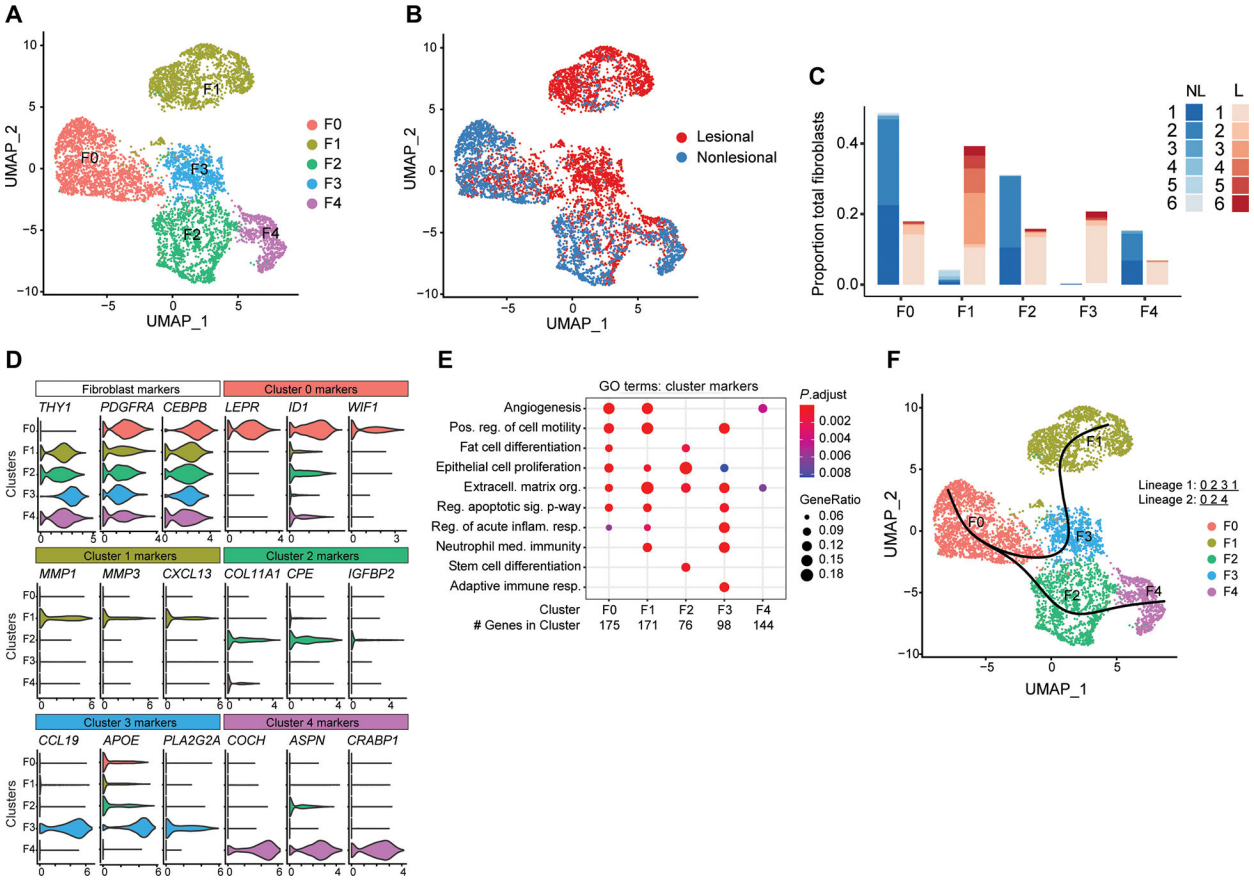

Fig. 1. scRNA-seq analysis of human acne lesions.

(**A**) UMAP plot of PDGFRA+ fibroblasts showing five distinct subtypes colored by cluster or (**B**) by disease association. (**C**) Stacked bar plot showing the donor and lesion type composition for each of the fibroblast cell types. Lesional cells (L) are shown in red, and nonlesional cells (NL) are shown in blue. (**D**) Violin plots of conserved pan-fibroblast marker gene expression and expression of major cluster markers for all five fibroblast subsets from the top three differentially expressed genes. (**E**) Dot plot of selected GO terms across all fibroblast subsets. Circle size corresponds to the proportion of markers annotated to a given term, while the fill color indicates the adjusted P value for the enrichment score. (**F**) Pseudotime analysis projected onto UMAP plot from (A). Curves represent inferred trajectories.

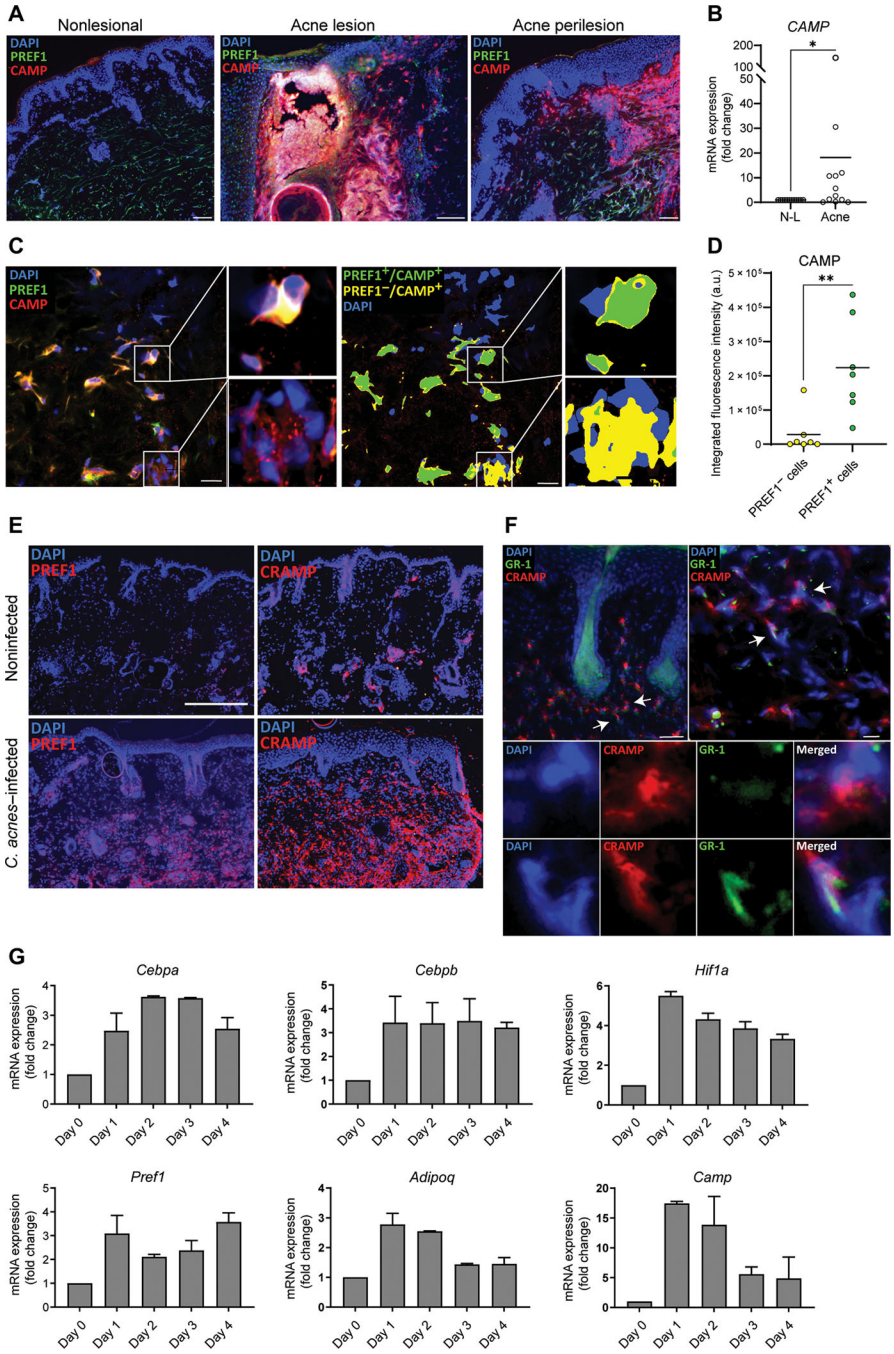

Fig. 2. Reactive adipogenesis occurs in the perifollicular stroma of acne.

(**A**) Representative immunofluorescence images from biopsy sections of human acne lesional and nonlesional skin stained for LL-37 (red), PREF1 (green), and 4′,6-diamidino-2-phenylindole (DAPI) (blue). Scale bars, 100 μm for nonlesional and perilesion and 150 μm for lesional skin. (**B**) RNA was extracted from tissue sections of 12 biopsies of eight acne patients, and *CAMP* mRNA expression from acne was measured by qPCR and normalized to nonlesional (N-L) skin. (**C**) Representative confocal microscopy image of the perifollicular dermis of an acne lesion stained for cathelicidin protein (CAMP),

PREF1, and DAPI, with higher magnification images provided from the boxed areas. Right panel shows the same representative image after thresholding, with green indicating areas where CAMP and PREF1 overlap and yellow color indicating areas where CAMP does not overlap with PREF1. (**D**) Quantification of the integrated fluorescence intensity of CAMP in overlapping and nonoverlapping PREF1-positive cells. Each spot represents a 212 μm × 212 μm perifollicular image from the dermis of acne lesions sampled from two patients. a.u., arbitrary units. (**E**) Representative immunofluorescence images of CAMP and PREF1 staining from skin biopsies of SKH-1 mice that were intradermally infected with *C. acnes* or noninfected after 7 days. (**F**) Representative immunofluorescence images of CRAMP, GR-1, and DAPI in the perifollicular area of SKH-1 mouse skin infected with *C. acnes*. White arrows indicate examples of CAMP-expressing cells that are positive or negative for GR-1 expression, with corresponding higher magnification images provided in the lower panel. Scale bar, 100 μm. (**G**) *C. acnes*–infected and noninfected SKH-1 mouse skin biopsies were collected on indicated days, and mRNA expression of the indicated genes was analyzed by qPCR with values shown relative to *Gapdh* control and normalized to noninfected (day 0) skin. $n = 3$ mice per condition. Data are means ± SEM. $*P < 0.05$ and $**P < 0.01$, two-tailed paired Student's *t* test.

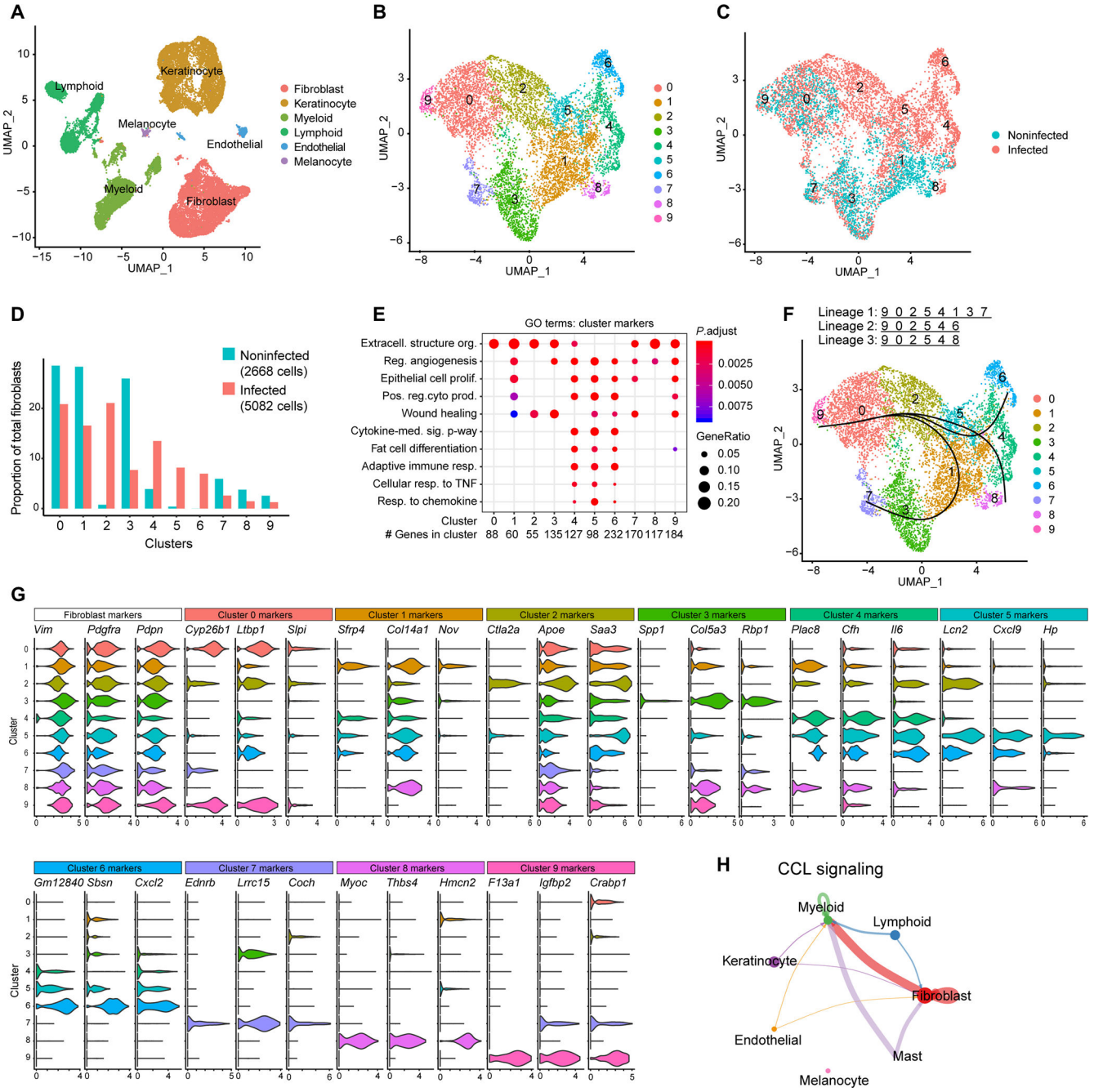

Fig. 3. scRNA-seq analysis of *C. acnes*–infected mouse skin reveals enrichment of adipogenic fibroblast subpopulations.

scRNA-seq was conducted on skin lesions 3 days after *C. acnes* infection or mock-infected control skin of SKH-1 mice. (**A**) UMAP plot of all cells passing initial quality control, showing cell type assignment based on established lineage markers. (**B**) UMAP plot after subclustering of *Pdgfra*$^{+}$ fibroblasts, showing 10 distinct subtypes (0 to 9) colored by cluster. (**C**) Subclustered fibroblasts colored by disease association. (**D**) Bar chart of the percentage of cells in each fibroblast cluster for *C. acnes*– and mock-infected skin. (**E**) Dot plot of selected GO terms across fibroblast clusters. Circle size corresponds to the proportion

of markers annotated to a given term, while the fill color indicates the adjusted *P* value for the enrichment score. (**F**) Pseudotime analysis projected onto UMAP plot from (A). Curves represent inferred trajectories. (**G**) Violin plots of conserved pan-fibroblast marker gene expression and expression of major cluster markers for all 10 fibroblast subsets from the top 3 differentially expressed genes. (**H**) CellChat circle plot of the CCL signaling pathway network. Edge color indicates sender. Edge weight is proportional to strength of communication signal. Circle sizes are proportional to the number of cells per cluster.

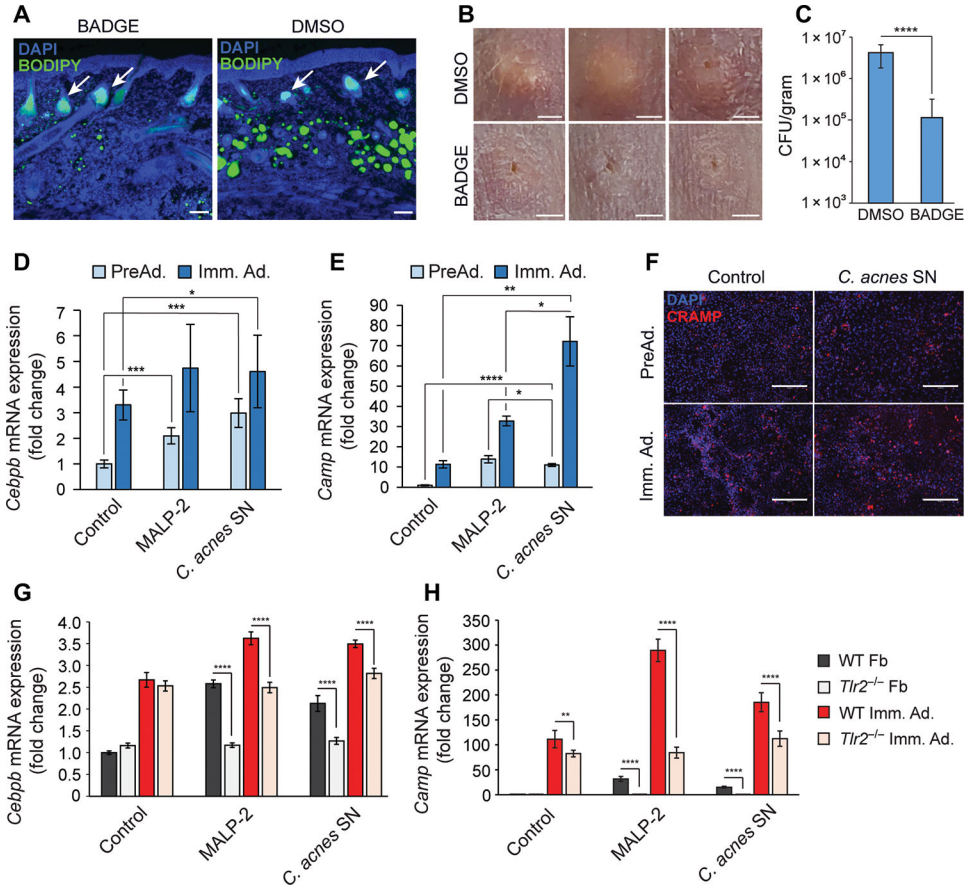

Fig. 4. *C. acnes* triggers adipocyte differentiation and *Camp* expression in dermal fibroblasts.

(**A** to **C**) SKH-1 mice were intraperitoneally injected daily with BADGE or vehicle (DMSO) as a control starting 1 day before intradermal infection with *C. acnes*. On day 6, skin was collected for analysis ($n = 5$). (A) Skin was stained with DAPI to stain nuclei or BODIPY to stain for the presence of lipid droplets. White arrows indicate sebaceous glands. Scale bar, 100 μm. (B) Representative images of the PBS control or *C. acnes* injection sites on mouse back after BADGE or DMSO vehicle treatment. Scale bar, 2 mm. (C) Enumeration of bacterial CFU from infected and mock-infected skin lesions of the infected area. (**D** and **E**) 3T3-L1 preadipocytes were cultured as nondifferentiated preadipocytes (PreAd.) or differentiated into immature adipocytes (Imm. Ad.) and stimulated for 24 hours with MALP-2 (100 ng/ml), 2.5% sterile conditioned *C. acnes* supernatant (SN), or bacterial culture medium (RCM) as control, and the relative mRNA expression of *Cebpb* (D) or *Camp* (E) was assessed by real-time qPCR. (**F**) Undifferentiated 3T3-L1 preadipocytes were stimulated with *C. acnes* SN for 48 hours, immunostained for CRAMP (red), and counterstained with DAPI (blue). Scale bar, 300 μm. (**G** and **H**) Primary dermal fibroblasts (Fb) isolated from wild-type (WT) or TLR2 knockout ($Tlr2^{-/-}$) mice were stimulated with MALP-2 (100 ng/ml), 2.5% *C. acnes* SN, or RCM control for 24 hours in the presence or absence of differentiation medium, and the relative mRNA expression of *Cebpb* (G) or *Camp* (H) was assessed by real-time qPCR. All data are means ± SD. $*P < 0.05$, $**P < 0.01$, $***P < 0.001$, and $****P < 0.0001$ using Student's paired *t* test.

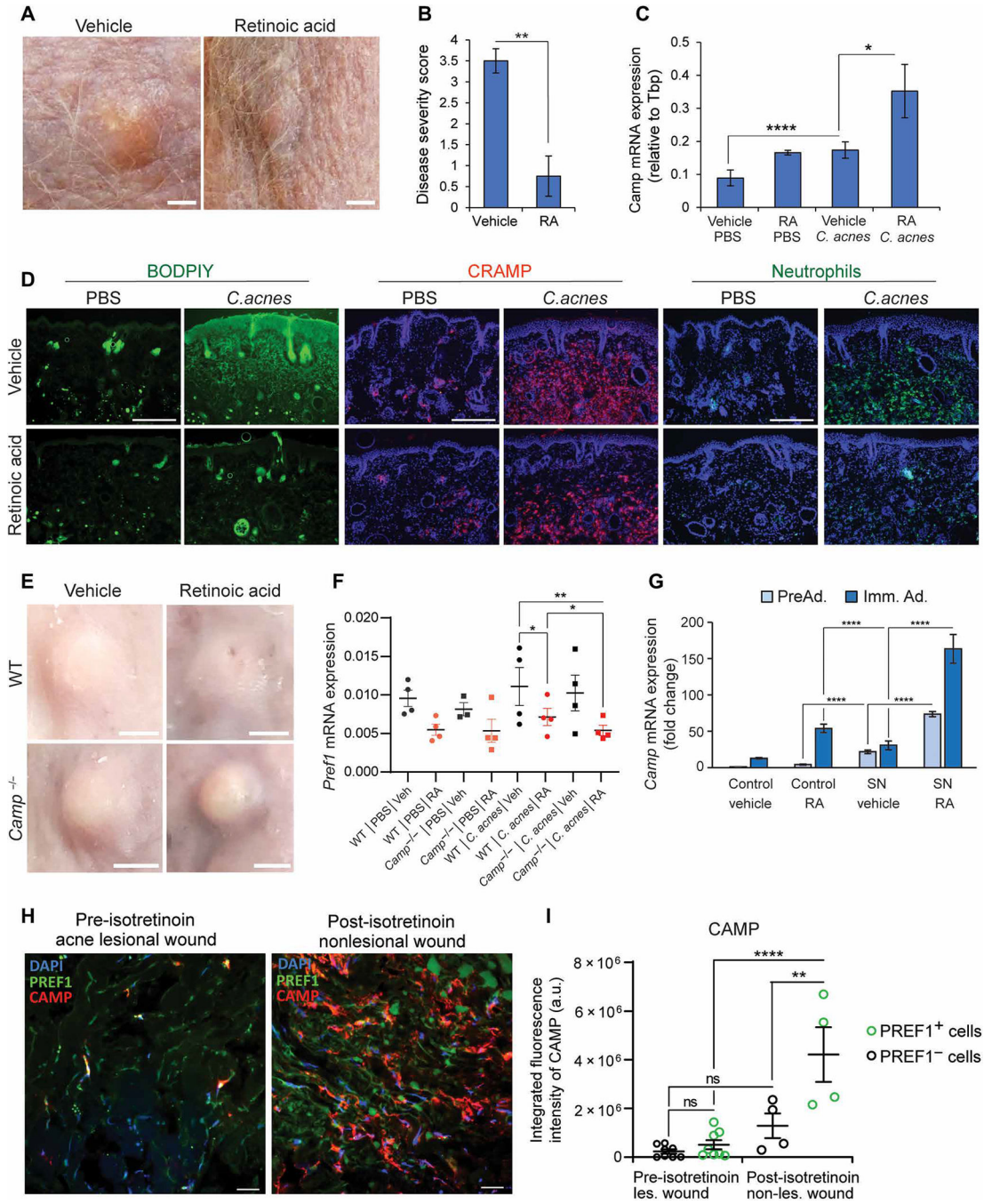

Fig. 5. RA inhibits adipogenesis and enhances cathelicidin in response to *C. acnes* infection.

SKH-1 mice were intradermally infected with *C. acnes* on day 0. Starting on day 3, mice were injected subcutaneously at a distal site with retinoic acid (RA) or olive oil (control) for 3 days ($n = 4$ per group). On day 6, skin was collected for analysis. (**A**) Representative day 6 images of acne-like lesions in mice treated with vehicle (left) or RA (right). Scale bar, 2 mm. (**B**) Disease severity score of *C. acnes*–infected lesions ($n = 4$) by investigator assessment of lesion severity ranging from 0 (no lesion detected) to 4 (most severe). (**C**) *Camp* mRNA expression in *C. acnes*–infected or mock PBS–infected mouse skin treated

with RA or vehicle control ($n = 4$ mice). (**D**) Fluorescent microscopy images of *C. acnes*–infected and mock PBS–infected mouse skin ($n = 4$), showing representative staining of total skin lipids (BODIPY dye, green), or immunolabeling of CRAMP (red) or neutrophils (anti–GR-1, green) for each treatment group (RA versus vehicle, $n = 4$ sections). All sections were counterstained with DAPI. Scale bar, 300 μm. (E and F) WT or *Camp*$^{-/-}$ C57BL/6 mice were intradermally infected with *C. acnes* and treated identically to SKH-1 mice listed above, and findings were assayed on day 6. (E) Representative day 6 images of acne-like lesions from WT and *Camp*$^{-/-}$ mice treated with vehicle (oil) or RA after injection with PBS control or infected with *C. acnes* (representative of 8 lesions, $n = 4$ mice per group, $n = 2$ lesions per mouse). Scale bar, 2 mm. (F) *C. acnes* lesions and control skin were collected on day 6, and mRNA was measured by qPCR for expression of *Pref1*. (G) 3T3-L1 preadipocytes were cultured as nondifferentiated preadipocytes (PreAd.) or differentiated into immature adipocytes (Imm. Ad.) and stimulated with 2.5% *C. acnes* SN or RCM control with or without 1 μM RA or vehicle (ethanol) controls for 24 hours, and the relative mRNA expression of *Camp* was assessed by qPCR. (H) Representative confocal images of dermal preadipocytes in 24-hour wounds from acne patients before and after isotretinoin therapy. Sections were stained for PREF1, CAMP, and DAPI, and thresholding was conducted on regions of CAMP staining with overlap of PREF1 and regions of CAMP staining without overlap of PREF1. Scale bar, 20 μm. (I) Quantification of the integrated fluorescence intensity of CAMP in PREF1-positive cells and PREF1-negative cells before and after isotretinoin treatment. Each spot represents a 212 μm × 212 μm perifollicular dermal image from acne sections from two acne patients. Data are means ± SEM. $*P < 0.05$, $**P < 0.01$, $***P < 0.001$, and $****P < 0.0001$ using Student's paired *t* test. Data in (I) represent means ± SEM with ordinary one-way ANOVA with Tukey's multiple comparisons test.